

Synthesis, Structure, and Dynamics of Six-Membered Metallocoronands and Metallodendrimers of Iron and Indium[‡]

Rolf W. Saalfrank,^{*,[a]} Christian Deutscher,^[a] Harald Maid,^[a] Ayuk M. Ako,^[a] Stefan Sperner,^[a] Takayuki Nakajima,^[a] Walter Bauer,^[a] Frank Hampel,^[a] Bernd A. Heß,^[b] Nico J. R. van Eikema Hommes,^[c] Ralph Puchta,^[c] and Frank W. Heinemann^[d]

In memoriam Professor Dieter Sellmann

Abstract: In the reaction of the *N*-substituted diethanolamines (H₂L¹⁻³) (**1–3**) with calcium hydride followed by addition of iron(III) or indium(III) chloride, the iron wheels [Fe₆Cl₆(L¹)₆] (**4**) and [Fe₆Cl₆(L²)₆] (**6**) or indium wheels [In₆Cl₆(L¹)₆] (**5**), [In₆Cl₆(L²)₆] (**8**) and [In₆Cl₆(L³)₆] (**9**) were formed in excellent yields. Exchange of the chloride ions of **6** by thiocyanate ions afforded [Fe₆(SCN)₆(L²)₆] (**7**). Whereas the structures of **4**, **5** and **7** were deter-

mined unequivocally by single-crystal X-ray analyses, complexes **8** and **9** were characterised by NMR spectroscopy. Contrary to what is normally presumed, the scaffolds of six-membered metallic wheels are not generally rigid,

Keywords: dendrimers · density functional calculations · indium · iron · NMR spectroscopy · supramolecular chemistry

but rather undergo nondissociative topomerisation processes. This was shown by variable temperature (VT) ¹H NMR spectroscopy for the indium wheel [In₆Cl₆(L¹)₆] (**5**) and is highlighted for the enantiotopomerisation of one indium centre {¹/₆[S₆-5] ↔ ¹/₆[S₆-5']}. The self-assembly of metallic wheels, starting from diethanolamine dendrons, is an efficient strategy for the convergent synthesis of metallodendrimers.

Introduction

Since the discovery that, below a critical temperature, paramagnetic molecular clusters can act as nanoscale magnets, the syntheses of polyoxometalates have become the focus of intense research activities. Such single-molecule magnets (SMMs) can be regarded as ideal model systems for the infinite-size version of the linear Heisenberg chain and are promising new materials for data storage and quantum computing. They exhibit magnetisation hysteresis, quantum tunnelling of magnetisation and, most interestingly, demonstrate an exciting effect: cooling by adiabatic magnetisation.^[1,2] Over the past years, considerable progress has been made towards the predictability of ordered supramolecular assemblies on the basis of coordinative metal/ligand bonds.^[3,4] A particular symmetric class are the so-called ferric wheels.^[4-6]

We have reported the template-mediated self assembly of six- and eight-membered iron coronates [NaC{Fe₆[N(CH₂-CH₂O)₃]₆}Cl and [CsC{Fe₈[N(CH₂CH₂O)₃]₈}Cl, prepared from triethanolamine with iron(III) chloride and sodium hydride or cesium carbonate.^[2,6] A common feature of these two complexes is that six or eight ethanolate arms solely function as ligands for the coordinative saturation of the

[a] Prof. Dr. R. W. Saalfrank, Dr. C. Deutscher, Dr. H. Maid, M. Sc. A. M. Ako, Dipl.-Chem. S. Sperner, Dr. T. Nakajima, Prof. Dr. W. Bauer, Dr. F. Hampel
Institut für Organische Chemie
Universität Erlangen-Nürnberg
Henkestrasse 42, 91054 Erlangen (Germany)
Fax: (+49)9131-852-1165
E-mail: saalfrank@chemie.uni-erlangen.de

[b] Prof. Dr. B. A. Heß
Lehrstuhl für Theoretische Chemie
Universität Erlangen-Nürnberg
Egerlandstrasse 3, 91058 Erlangen (Germany)

[c] Dr. N. J. R. van Eikema Hommes, Dr. R. Puchta
Computer-Chemie-Centrum
Universität Erlangen-Nürnberg
Nägelsbachstrasse 25, 91052 Erlangen (Germany)

[d] Dr. F. W. Heinemann
Institut für Anorganische Chemie
Universität Erlangen-Nürnberg
Egerlandstrasse 1, 91058 Erlangen (Germany)

[‡] Chelate complexes (metallocoronands), Part 26. Part 25: R. W. Saalfrank, U. Reimann, F. Hampel, C. Goebel, R. Herbst-Irmer, *Z. Naturforsch. Teil. B* **2003**, *58*, 22–26.

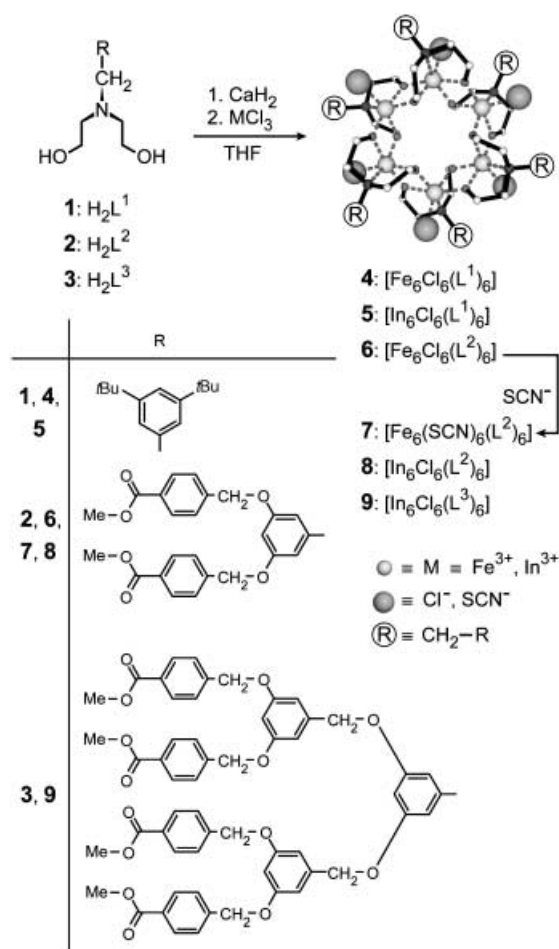
iron centres and for charge compensation, whereas the remaining ethanolate μ_2 -O donors are structure-determining. They are linkers, necessary for the ring formation. Consequently, reaction of *N*-butyl-diethanolamine with calcium hydride and iron(III) chloride yielded the unoccupied neutral iron coronand $[\text{Fe}_6\text{Cl}_6\{\text{BuN}(\text{CH}_2\text{CH}_2\text{O})_2\}_6]$.^[4] In this case, completion of the octahedral coordination sphere at iron and charge compensation are achieved by the chloride co-ligands.

Results and Discussion

In order to test scope and limitation of this new synthesis for six-membered iron wheels, we treated *N*-(3,5-bis-*tert*-butylbenzyl)diethanolamine (**1**; H_2L^1) with calcium hydride and iron(III) chloride and isolated a yellow microcrystalline product. The elemental analysis and FAB-MS spectrum identified **4** as a hexairon chelate complex of the composition $[\text{Fe}_6\text{Cl}_6(\text{L}^1)_6]$ (Scheme 1).

For an unambiguous characterisation of $[\text{Fe}_6\text{Cl}_6(\text{L}^1)_6]$ (**4**), we carried out an X-ray crystallographic structure analysis.^[7–9] Principally, complex **4** is isostructural with the six-membered ferric wheel $[\text{Fe}_6\text{Cl}_6\{\text{BuN}(\text{CH}_2\text{CH}_2\text{O})_2\}_6]$. That is to say, the twelve ethanolate μ_2 -O donors of $(\text{L}^1)^{2-}$, together with the six iron(III) ions form the ring, and the six chloride ions again are only necessary for charge compensation and as co-ligands for an octahedral environment at iron. The iron wheel **4** (Figure 1) crystallises with three molecules in the unit cell and the disklike clusters are piled in cylindrical columns with mean intra-columnar midpoint distances d of 13.7 Å, with all the iron centres superimposed. Each column is surrounded by six parallel columns, which are alternately dislocated by $1/3 d$ and $2/3 d$ against the central one.

When ligand **1** was treated with calcium hydride and indium(III) chloride instead of iron(III) chloride, we isolated the corresponding indium wheel $[\text{In}_6\text{Cl}_6(\text{L}^1)_6]$ (**5**) (Scheme 1). Single-crystal X-ray analysis proved **5**^[10] to be isostructural with iron wheel **4**. In the solid state, the *N*-substituted diethanolamine ligands of S_6 -**5** are desymmetrised through metal coordination. That **5** is the only species present also in solution was demonstrated by ESI mass spectroscopy ($m/z = 2753$ for $[\text{In}_6\text{Cl}_5(\text{L}^1)_6 \cdot 3\text{H}_2\text{O}]^+$ in toluene). At temperatures below 50 °C, a “static” S_6 -symmetric structure is observed by ¹H and ¹³C NMR spectroscopy. All ¹H and ¹³C NMR resonances were unambiguously assigned by a combination of COSY, HMQC, and HMBC spectra. Exemplarily, the most significant ¹H NMR characteristics of **5** are discussed (Figure 2). A major feature of the desymmetrised $(\text{L}^1)^{2-}$ ligands is the diastereotopicity of the 12 ethanolate arms



Scheme 1. Synthesis of $[\text{Fe}_6\text{Cl}_6(\text{L}^1)_6]$ (**4**), $[\text{In}_6\text{Cl}_6(\text{L}^1)_6]$ (**5**), $[\text{Fe}_6\text{Cl}_6(\text{L}^2)_6]$ (**6**), $[\text{Fe}_6(\text{SCN})_6(\text{L}^2)_6]$ (**7**), $[\text{In}_6\text{Cl}_6(\text{L}^2)_6]$ (**8**) and $[\text{In}_6\text{Cl}_6(\text{L}^3)_6]$ (**9**).

and, as a result, the formation of a set of four distinguishable methylene groups, which like the six *N*-benzylic methylene groups exhibit the characteristic AB splitting patterns for their diastereotopic methylene protons. In contrast, the

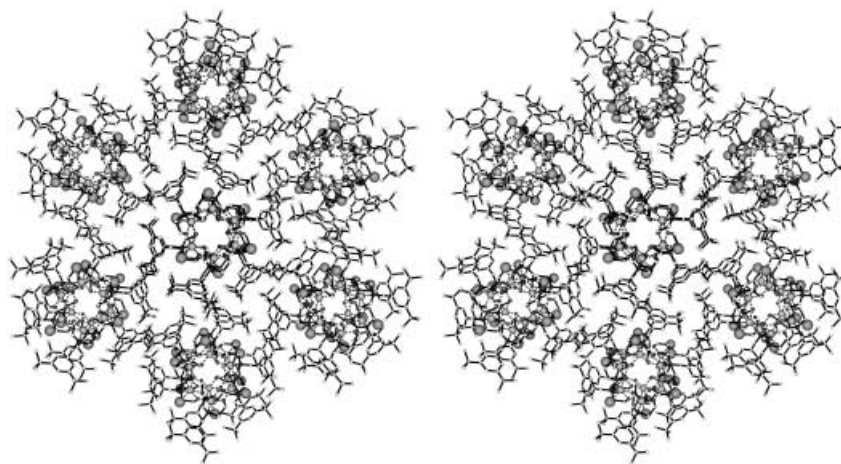


Figure 1. (Stereo view): Structure of $[\text{Fe}_6\text{Cl}_6(\text{L}^1)_6]$ (**4**) in the crystal, highlighting the packing of seven parallel columns, with six columns alternately dislocated by $1/3 d$ and $2/3 d$ against a central one. Solvent molecules and hydrogen atoms are not depicted for clarity.

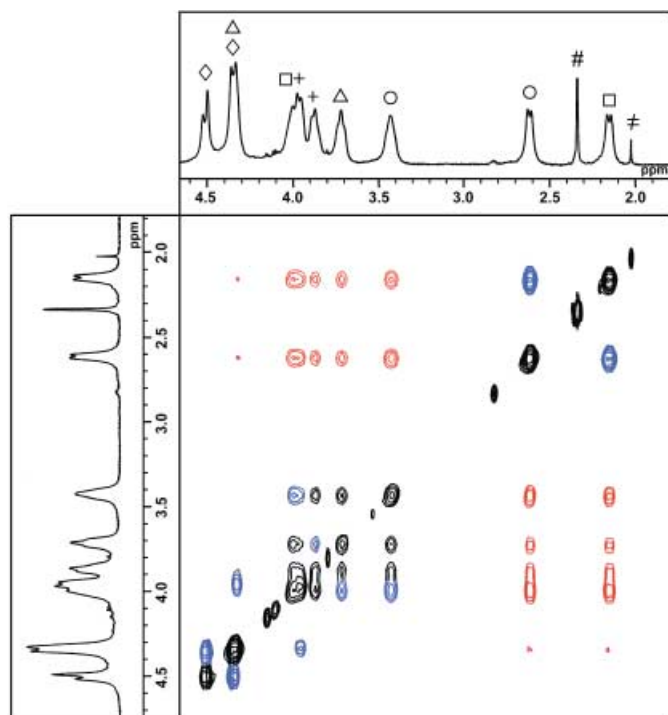


Figure 2. $^1\text{H},^1\text{H}$ -EXSY spectrum of $[\text{In}_6\text{Cl}_6(\text{L}^1)_6]$ (**5**) (CDCl_3 , 30°C). Correlation of the signals: ethanolate arms: OCH_2 ($\Delta, +$), NCH_2 (\square, \circ); benzylic groups: NCH_2 (\diamond). Each geminal pair of protons is assigned with identical symbols. A phase sensitive ROESY-sequence has been employed, mixing time 300 ms. Cross peaks highlighted in red are ROE peaks. Other cross peaks are exchange peaks (blue) and TOCSY peaks (black). H_2O (#); acetone (\neq).

12 *t*Bu groups and the pairs of aromatic protons, *ortho* to the CH_2N link, are homotopic due to free rotation of the aromatic rings.

Variable temperature ^1H NMR studies on the enantiotopomerisation of tetrahedral homochiral ($\Delta, \Delta, \Delta, \Delta$)- $[(\text{NH}_4)_4\cap\{\text{Mg}_4(\text{L})_6\}]^{\pm} \rightleftharpoons (\Lambda, \Lambda, \Lambda, \Lambda)$ - $[(\text{NH}_4)_4\cap\{\text{Mg}_4(\text{L})_6\}]$ ($\text{L} =$ diethyl ketipinate dianion)^[11] prompted us to also study the dynamic behaviour of $[\text{In}_6\text{Cl}_6(\text{L}^1)_6]$ (**5**) by VT NMR spectroscopy.^[12] At higher temperatures in $[\text{D}_5]$ bromobenzene, the diastereotopic protons of the five distinguishable methylene groups, undergo pairwise mutual exchange. This phenomenon clearly manifested already at temperatures below 50°C in chloroform in exchange cross peaks in EXSY-type spectra (Figure 2). The off-diagonal signals represent three different types of cross peaks: ROE-signals, which indicate spatial relationship (opposite phase as diagonal signals, depicted in red), TOCSY-type signals, indicating scalar coupling (same phase as diagonal signals, black), and exchange signals (same phase as diagonal signals, blue).

The high-temperature ^1H NMR spectra (Figure 3) indicate time-averaged pseudo- D_{3d} molecular symmetry for **5** due to rapid, nondissociative topomerisation of bistable S_6 -**5** with a fast S_6 -**5** $\rightleftharpoons S_6$ -**5'** interconversion. As explicitly shown for the benzylic diastereotopic protons of **5**, coalescence is observed at 130°C (500 MHz). The activation parameters for the molecular interconversion have been derived from a line shape analysis: $\Delta H^\ddagger = 9.0 \text{ kcal mol}^{-1}$, $\Delta S^\ddagger = -27 \text{ cal K}^{-1} \text{ mol}^{-1}$, $\Delta G_{403}^\ddagger = 20.0 \text{ kcal mol}^{-1}$.

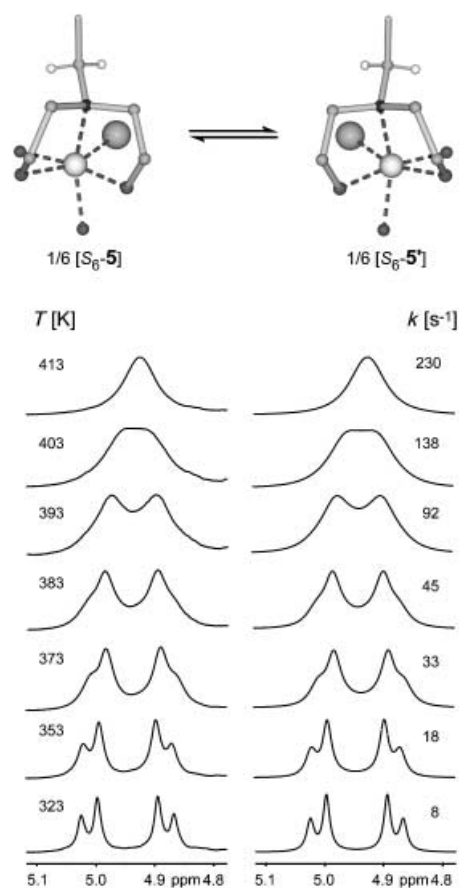


Figure 3. Enantiotopomerisation of one indium centre of **5** ($1/6 [S_6\text{-5}] \rightleftharpoons 1/6 [S_6\text{-5}']$) leading to enantiotopomerisation of the diastereotopic groups of ligand $(\text{L}^1)^{2-}$. For clarity only the VT ^1H NMR signals of the benzylic methylene protons of the topomerisation of **5** are depicted. Left: experimental (500 MHz, $\text{C}_6\text{D}_5\text{Br}$); right: simulated.

Density functional calculations at B3LYP/LANL2DZp^[13–16] and BP86/RI/SV(P)^[17–20] on a model compound $[\text{In}_6\text{Cl}_6\{\text{MeN}(\text{CH}_2\text{CH}_2\text{O})_2\}_6]$ (**MC**), in which the *N*-(3,5-bis-*tert*-butylbenzyl) groups of **5** have been replaced by *N*-methyl groups suggest that an $S_6\text{-MC} \rightleftharpoons S_6\text{-MC}'$ interconversion does not involve a highly symmetrical transition structure. The obvious transition state $D_{3d}\text{-MC}$, in which enantiotopomerisation proceeds synchronously at all indium centres, turns out to be a hilltop structure with three imaginary frequencies, $36.1 \text{ kcal mol}^{-1}$ less stable than the ground state $S_6\text{-MC}$. The favoured transition structure has approximate C_s symmetry, $[C_s\text{-MC}]^\ddagger$, and corresponds to an activation barrier of $16.6 \text{ kcal mol}^{-1}$. The imaginary mode indicates that the topomerisation proceeds in a concerted, yet asynchronous fashion (Figure 4). A calculation on the full complex $[\text{In}_6\text{Cl}_6(\text{L}^1)_6]$ (**5**) on BP86/RI/SV(P) level with a 46-electron pseudopotential yields a C_s structure $20.9 \text{ kcal mol}^{-1}$ above the S_6 ground state, whereas the D_{3d} stationary point is found to be $44.6 \text{ kcal mol}^{-1}$ less stable than the ground state.

The significant scope of the synthesis of six-membered metallic wheels starting from alkyl-substituted diethanolamines was further demonstrated in reacting branched dendritic diethanolamines H_2L^2 (**2**) and H_2L^3 (**3**)^[21] with calcium

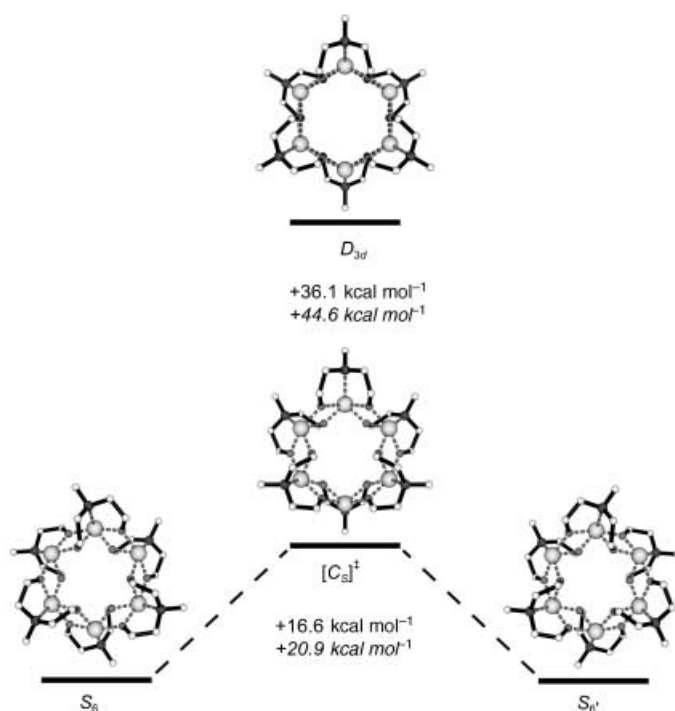


Figure 4. Pictogram and energy values, illustrating the topomerisation of **MC** and **5** in a concerted, yet asynchronous fashion. The D_{3d} structure in which enantiotopomerisation proceeds synchronously at all indium centres turns out to be a hilltop structure. Energy values given in italic correspond to **5**.

hydride and iron(III)/indium(III) chloride. The elemental analyses and FAB-MS spectra identified the reaction products as the hexametallate complexes $[\text{Fe}_6\text{Cl}_6(\text{L}^2)_6]$ (**6**), $[\text{In}_6\text{Cl}_6(\text{L}^2)_6]$ (**8**), and $[\text{In}_6\text{Cl}_6(\text{L}^3)_6]$ (**9**) (Scheme 1). In order to grow single-crystals suitable for an X-ray analysis, $[\text{Fe}_6\text{Cl}_6(\text{L}^2)_6]$ (**6**) was transformed with rhodanide ions to give $[\text{Fe}_6(\text{SCN})_6(\text{L}^2)_6]$ (**7**) (Scheme 1, Figure 5).^[22] According to this analysis, **7** is isostructural with $[\text{Fe}_6\text{Cl}_6(\text{L}^1)_6]$ (**4**).

For unambiguous characterisation of $[\text{In}_6\text{Cl}_6(\text{L}^2)_6]$ (**8**) and $[\text{In}_6\text{Cl}_6(\text{L}^3)_6]$ (**9**) we carried out ^1H and ^{13}C NMR spectra. Exemplarily, the most significant ^1H NMR characteristics are discussed for **9** (Figure 6). A major feature of the $(\text{L}^3)^{2-}$ ligands, desymmetrised through metal coordination, is the loss of chemical-shift differences of diastereotopic protons towards the periphery of the dendrimer. The diastereotopic protons of the methylene groups of the ethanolate arms and

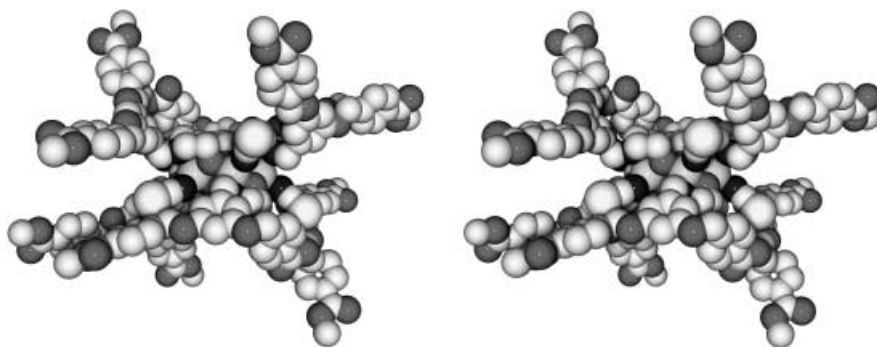


Figure 5. Stereoview of crystal structure of metallo dendrimer $[\text{Fe}_6(\text{SCN})_6(\text{L}^2)_6]$ (**7**).

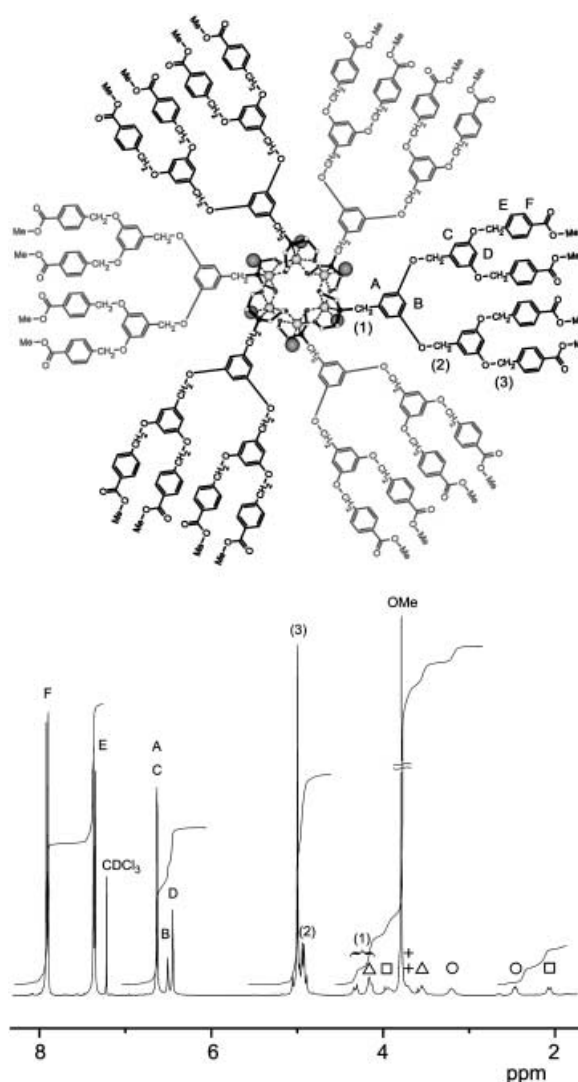


Figure 6. ^1H NMR spectrum (CDCl_3 ; 21°C) of metallo dendrimer $[\text{In}_6\text{Cl}_6(\text{L}^3)_6]$ (**9**) and correlation of the signals. Ethanolate arms: OCH_2 (Δ , $+$), NCH_2 (\square , \circ); benzylic groups: NCH_2 (1); inner OCH_2 (2); peripheral OCH_2 (3). Aromatic protons are marked as A–F.

the *N/O*-benzylic protons (1,2) give rise to six discernible AB splitting patterns. The assignment of these signals is based on NMR experiments as carried out for **5**. By contrast, the diastereotopic protons within the 24 peripheral *O*-benzylic methylene groups (3) coincide and lead to only one signal for the 48 protons. Naturally, due to rotation of the phenyl groups, the pairs of aromatic protons (A,C,E,F) are isochronous. For the same reason, all CH_3 resonances result in a singlet for the 72 protons involved.

Conclusion

Provided that the bridging ligands are flexible, metallacoro-

nands are not necessarily rigid. This was demonstrated by temperature-dependent ^1H NMR spectroscopy for a diamagnetic indium analogue. In summary, the six indium centres experience inversion of configuration resulting in retention of the overall S_6 molecule symmetry. Calculations indicate that the topomerisation proceeds in a concerted, yet asynchronous fashion. Advanced studies towards metallodendrimers^[23] are on the way.

Experimental Section

NMR-spectra were recorded on JEOL Alpha 500, JEOL EX 400 and JEOL GX 400 spectrometers. Solvent signals were employed as internal standards: CDCl_3 (^1H , 7.24 ppm; ^{13}C , 77.0 ppm); $\text{C}_6\text{D}_5\text{Br}$ (^1H , 7.17 ppm; ^{13}C , 122.51 ppm).

Compounds 1–3: Syntheses according to standard methods from the corresponding bromide and dendritic bromides^[21] with diethanolamine.

Compounds 4–9

General procedure: Either H_2L^1 (**1**) (0.62 g, 2.0 mmol) for **4** and **5**, H_2L^2 (**2**) (1.05 g, 2.0 mmol) for **6** and **8**, or H_2L^3 (**3**) (2.13 g, 2.0 mmol) for **9** was added to a suspension of calcium hydride (0.13 g, 3.0 mmol) in anhydrous THF (125 mL). After the suspension was stirred for 1 h at 20°C, a solution of either iron(III) chloride (0.32 g, 2.0 mmol) for **4** and **6**, or indium(III) chloride (0.44 g, 2.0 mmol) for **5**, **8** and **9** in anhydrous THF (50 mL) was added. The reaction mixture was stirred at 20°C for 72 h, then the solvent was removed under vacuum. The precipitate was dissolved in CH_2Cl_2 (100 mL) and the remaining residue was filtered off. After evaporation of the solvent **4** and **6** were obtained as yellow and **5**, **8** and **9** as white powders.

Rhodanide **7** was prepared by exchange of the co-ligand Cl^- by SCN^- .^[24]

Compound 4: Yield 0.34 g, 43% (yellow rhombic crystals from toluene at 4°C; m.p. >240°C (decomp); FAB-MS (3-NBA): m/z (%): 1552 (30) $[\text{Fe}_6\text{Cl}_6(\text{L}^1)_6]^+$, 1190 (40) $[\text{Fe}_3\text{Cl}_3(\text{L}^1)_3]^+$, 1155 (40) $[\text{Fe}_3\text{Cl}_2(\text{L}^1)_3]^+$, 1119 (100) $[\text{Fe}_3\text{Cl}(\text{L}^1)_3]^+$; IR (KBr): $\tilde{\nu}$ =2965, 2906, 2867, 1600, 1477, 1461, 1088, 729 cm^{-1} ; elemental analysis calcd (%) for $\text{C}_{114}\text{H}_{186}\text{Cl}_6\text{Fe}_6\text{N}_6\text{O}_{12}$: toluene (2472.70): C 58.78, H 7.91, N 3.40; found: C 58.70, H 8.16, N 3.38.

Compound 5: Yield 0.32 g, 35% (colourless rhombic crystals from toluene at 4°C; m.p. >240°C (decomp); ^1H NMR (500.1 MHz, $\text{C}_6\text{D}_5\text{Br}$, 50°C): δ =7.725 (s, 12H; aryl), 7.696 (s, 6H; aryl), 5.013 (d, J =13.8 Hz, 6H; benzyl), 4.882 (d, J =13.8 Hz, 6H; benzyl), 4.621 (dd, J =5.0, 10.6 Hz, 6H; O- CH_2), 4.510 (dt, J =6.4, 12.9 Hz, 6H; N- CH_2), 4.228 (dd, J =6.2, 11.5 Hz, 6H; O- CH_2), 4.102 (dd, J =5.3, 10.3 Hz, 6H; O- CH_2), 3.844 (dt, J =2.8, 11.5 Hz, 6H; N- CH_2), 3.776 (dt, J =5.9, 11.7 Hz, 6H; O- CH_2), 2.822 (d, J =9.8 Hz, 6H; N- CH_2), 2.286 (d, J =11.2 Hz, 6H; N- CH_2), 1.565 ppm (s, 108H; *t*Bu); ^{13}C NMR (125.7 MHz, CDCl_3 , 25°C): δ =150.47 (12C, quat. aryl), 132.39 (6C, quat. aryl), 125.87 (12C, CH aryl), 121.69 (6C, CH aryl), 62.66 (6C, benzyl), 61.77 (6C, O- CH_2), 60.13 (6C, O- CH_2), 58.08 (6C, N- CH_2), 55.71 (6C, N- CH_2), 34.75 (12C, CMe_3), 31.51 ppm (36C, Me); ESI-MS: m/z (%): 2753 (100) $[\text{In}_6\text{Cl}_6(\text{L}^1)_6]^+$, 2698 (8) $[\text{In}_6\text{Cl}_5(\text{L}^1)_6]^+$, 1787 (80) $[\text{In}_4\text{Cl}_3(\text{L}^1)_4]^+$, 1330 (80) $[\text{In}_3\text{Cl}_2(\text{L}^1)_3]^+$, 875 (100) $[\text{In}_2\text{Cl}(\text{L}^1)_2]^+$; IR (KBr): $\tilde{\nu}$ =2965, 2870, 1602, 1477, 1460, 1079, 715 cm^{-1} ; elemental analysis calcd (%) for $\text{C}_{114}\text{H}_{186}\text{Cl}_6\text{In}_6\text{N}_6\text{O}_{12}$: THF (2806.51): C 50.50, H 6.97, N 2.99; found: C 50.51, H 6.96, N 2.88.

Compound 6: Yield 0.70 g, 57% (yellow thin needles from chloroform by diffusion of diethyl ether at 20°C; m.p. >240°C (decomp); FAB-MS (3-NBA): m/z (%): 3677 (10) $[\text{Fe}_6\text{Cl}_6(\text{L}^2)_6]^+$, 3640 (68) $[\text{Fe}_6\text{Cl}_5(\text{L}^2)_6]^+$, 2415 (75) $[\text{Fe}_4\text{Cl}_3(\text{L}^2)_4]^+$, 1767 (100) $[\text{Fe}_3\text{Cl}(\text{L}^2)_3]^+$; IR (KBr): $\tilde{\nu}$ =2947, 2913, 2866, 1721, 1601, 1445, 1281, 1154, 1109 cm^{-1} ; elemental analysis calcd (%) for $\text{C}_{174}\text{H}_{186}\text{Cl}_6\text{Fe}_6\text{N}_6\text{O}_{48}$ (3677.20): C 56.83, H 5.10, N 2.29; found: C 56.10, H 5.29, N 2.17.

Compound 7: Yield 0.59 g, 81% (orange crystals from chloroform by diffusion of diethyl ether at 20°C; m.p. >240°C (decomp); FAB-MS (3-NBA): m/z (%): 3755 (10) $[\text{Fe}_6(\text{SCN})_5(\text{L}^2)_6]^+$, 2483 (50) $[\text{Fe}_4(\text{SCN})_3(\text{L}^2)_4]^+$, 2425 (100) $[\text{Fe}_2(\text{SCN})_2(\text{L}^2)_2]^+$, 2368 (50) $[\text{Fe}_2(\text{SCN})(\text{L}^2)]^+$; IR (KBr): $\tilde{\nu}$ =2926, 2077, 2041, 1720, 1620, 1287 cm^{-1} ;

elemental analysis calcd (%) for $\text{C}_{180}\text{H}_{186}\text{Fe}_6\text{N}_{12}\text{O}_{48}\text{S}_6\cdot 2\text{CHCl}_3$ (4051.73): C 53.95, H 4.68, N 4.15, S 4.75; found: C 54.65, H 5.27, N 4.05, S 4.43.

Compound 8: Yield 0.69 g, 51% (colourless microcrystals from acetone/ CHCl_3 50:1, at 4°C; m.p. >240°C (decomp); ^1H NMR (400.1 MHz, CDCl_3 , 22°C): δ =8.00 (d, J =8.4 Hz, 24H; aryl), 7.48 (d, J =8.4 Hz, 24H; aryl), 6.69 (d, J =2.1 Hz, 12H; aryl), 6.58 (t, J =2.1 Hz, 6H; aryl), 5.13 (d, J =13.4 Hz, 12H; benzyl-O), 5.10 (d, J =13.6 Hz, 12H; benzyl-O), 4.40 (d, J =13.6 Hz, 6H; benzyl-N), 4.03–4.23 (m, 12H; benzyl-N, CH_2 - CH_2 -O), 3.89 (d, 6H; J =11.7 Hz, N- CH_2), 3.85 (s, 36H; O- CH_3), 3.75–3.81 (m, 12H; CH_2 - CH_2 -O), 3.59–3.66 (m, 6H; CH_2 - CH_2 -O), 3.28–3.30 (m, 6H; N- CH_2), 2.53 (d, J =9.8 Hz, 6H; N- CH_2), 2.01 ppm (d, J =11.8 Hz, 6H; N- CH_2); ^{13}C NMR (100.5 MHz, CDCl_3 , 23°C): δ =166.7 (12C, C=O), 159.3 (12C, quat. aryl), 141.9 (12C, quat. aryl), 135.6 (6C, quat. aryl), 129.8 (24C, CH aryl), 129.7 (12C, quat. aryl), 127.4 (24C, CH aryl), 110.7 (12C, CH aryl), 102.4 (6C, CH aryl), 69.4 (12C, benzyl-O), 62.5 (6C, benzyl-N), 61.8 (6C, CH_2 - CH_2 -O), 60.1 (6C, CH_2 - CH_2 -O), 58.5 (6C, N- CH_2), 55.9 (6C, N- CH_2), 52.1 (12C, O- CH_3); FAB-MS (3-NBA): m/z (%): 4053 (1) $[\text{In}_6\text{Cl}_6(\text{L}^2)_6 + \text{Na}]^+$, 2201 (10) $[\text{In}_4\text{Cl}_5(\text{L}^2)_5]^+$, 2016 (10) $[\text{In}_3\text{Cl}_3(\text{L}^2)_3]^+$, 1529 (30) $[\text{In}_3\text{Cl}_4(\text{L}^2)_2]^+$, 1343 (25) $[\text{In}_2\text{Cl}_2(\text{L}^2)_2]^+$, 1272 (100) $[\text{In}_2(\text{L}^2)_2]^+$; IR (KBr): $\tilde{\nu}$ =2951, 2873, 1724, 1597, 1436, 1283, 1157, 757 cm^{-1} ; elemental analysis calcd (%) for $\text{C}_{174}\text{H}_{186}\text{Cl}_6\text{In}_6\text{N}_6\text{O}_{48}\cdot 3\text{CHCl}_3$ (4389.16): C 48.44, H 4.34, N 1.92; found: C 48.39, H 4.72, N 1.88.

Compound 9: Yield 1.07 g, 44% (colourless microcrystals from acetone/ CHCl_3 50:1, at 4°C; m.p. >240°C (decomp); ^1H NMR (400.1 MHz, CDCl_3 , 21°C): δ =7.93 (d, J =8.3 Hz, 48H; aryl), 7.38 (d, J =8.3 Hz, 48H; aryl), 6.64–6.66 (m, 36H; aryl), 6.53 (s, 6H; aryl), 6.47 (t, J =2.1 Hz, 12H; aryl), 5.02 (s, 48H; benzyl-O), 4.97 (d, J =12.3 Hz, 12H; benzyl-O), 4.94 (d, J =12.1 Hz, 12H; benzyl-O), 4.35 (d, J =12.1 Hz, 6H; benzyl-N), 4.12–4.18 (m, 12H; benzyl-N, CH_2 - CH_2 -O), 3.96–4.00 (m, 6H; N- CH_2), 3.82 (s, 72H; O- CH_3), 3.64–3.78 (m, 12H; CH_2 - CH_2 -O), 3.52–3.58 (m, 6H; CH_2 - CH_2 -O), 3.19–3.26 (m, 6H; N- CH_2), 2.48 (d, 6H; J =8.5 Hz, N- CH_2), 2.09 ppm (d, 6H; J =11.1 Hz, N- CH_2); ^{13}C NMR (100.5 MHz, CDCl_3 , 23°C): δ =166.7 (24C, C=O), 159.8 (24C, quat. aryl), 159.4 (12C, quat. aryl), 141.8 (24C, quat. aryl), 139.4 (12C, quat. aryl), 135.4 (6C, quat. aryl), 129.8 (48C, CH aryl), 129.6 (24C, quat. aryl), 126.9 (48C, CH aryl), 110.6 (12C, CH aryl), 106.6 (24C, CH aryl), 102.1 (6C, CH aryl), 101.5 (12C, CH aryl), 69.8 (12C, benzyl-O), 69.3 (24C, benzyl-O), 62.6 (6C, benzyl-N), 61.9 (6C, CH_2 - CH_2 -O), 60.1 (6C, CH_2 - CH_2 -O), 58.6 (6C, N- CH_2), 56.0 (6C, N- CH_2), 52.1 ppm (24C, O- CH_3); FAB-MS (3-NBA): m/z (%): 7275 (1) $[\text{In}_6\text{Cl}_6(\text{L}^3)_6]^+$, 7241 (1) $[\text{In}_6\text{Cl}_5(\text{L}^3)_6]^+$, 3530 (82) $[\text{In}_5(\text{L}^3)_5]^+$, 2352 (100) $[\text{In}_2(\text{L}^3)_2]^+$; IR (KBr): $\tilde{\nu}$ =2956, 2926, 2874, 1744, 1605, 1263 cm^{-1} ; elemental analysis calcd (%) for $\text{C}_{366}\text{H}_{354}\text{Cl}_6\text{In}_6\text{N}_6\text{O}_{96}\cdot 3\text{CHCl}_3$ (7632.56): C 58.07, H 4.72, N 1.10; found: C 58.38, H 4.91, N 1.02.

Computational methods: Calculations were performed using the Gaussian 98^[13] and Turbomole 5.6^[17] program packages. We employed the B3LYP^[14] hybrid density functional and the BP86^[18] functional, the latter in connection with the resolution of the identity (RI) technique.^[19] In the B3LYP calculations, we used the Los Alamos LANL2DZ^[15] ECP basis set, as implemented in Gaussian 98, augmented with polarisation functions on the heavy atoms.^[16] In the BP86/RI computations, we used Ahlrichs' split valence basis set^[20] with polarisation functions on the heavy atoms and the 46e MWB ECP, as implemented in Turbomole 5.6.

Acknowledgement

This work was supported by the Deutsche Forschungsgemeinschaft (Sa 276/25–1, SFB 583, GK 312, SPP 1137), the Bayerisches Langzeitprogramm *Neue Werkstoffe* and the Fonds der Chemischen Industrie. T.N. thanks the Alexander von Humboldt Stiftung for a post doctoral fellowship. Prof. Dr. M. Schmittel, Organische Chemie I, Universität Siegen, is acknowledged for ESI spectrometry measurements. The generous allocation of X-ray facilities by Prof. D. Sellmann, Institut für Anorganische Chemie, Universität Erlangen-Nürnberg, is also gratefully acknowledged. We thank the Regionales Rechenzentrum Erlangen (RRZE) for a generous allotment of computer time.

- [1] V. Marvaud, C. Decroix, A. Scullier, C. Guyard-Duhayon, J. Vaiser-mann, F. Gonnet, M. Verdaguier, *Chem. Eur. J.* **2003**, *9*, 1677–1691; R. Sessoli, D. Gatteschi, *Angew. Chem.* **2003**, *115*, 278–309; *Angew. Chem. Int. Ed.* **2003**, *42*, 268–297; H. Oshio, N. H. Hoshino, T. Ito, M. Nakano, F. Renz, P. Gütllich, *Angew. Chem.* **2003**, *115*, 233–235; *Angew. Chem. Int. Ed.* **2003**, *42*, 223–225; L. F. Jones, A. Batsanov, E. K. Brechini, D. Collins, M. Helliwell, T. Mallah, E. J. L. McInnes, S. Piligos, *Angew. Chem.* **2002**, *114*, 4494–4497; *Angew. Chem. Int. Ed.* **2002**, *41*, 4318–4321; R. Koch, S. Schromm, J. Schülein, P. Müller, I. Bernt, R. W. Saalfrank, F. Hampel, E. Balthes, *Inorg. Chem.* **2001**, *40*, 2986–2995; A. Müller, F. Peters, M. T. Pope, D. Gatteschi, *Chem. Rev.* **1998**, *98*, 239–271; O. Waldmann, J. Schülein, R. Koch, P. Müller, I. Bernt, R. W. Saalfrank, H. P. Andres, H. U. Güdel, P. Allenspach, *Inorg. Chem.* **1999**, *38*, 5879–5886; R. W. Saalfrank, S. Trummer, U. Reimann, M. M. Chowdhry, F. Hampel, O. Waldmann, *Angew. Chem.* **2000**, *112*, 3634–3637; *Angew. Chem. Int. Ed.* **2000**, *39*, 3492–3494; D. Gatteschi, R. Sessoli, A. Cornia, *Chem. Commun.* **2000**, 725–732; E. Coronado, J. R. Galán-Mascarós, C.-J. Gómez-García, J. Ensling, P. Gütllich, *Chem. Eur. J.* **2000**, *6*, 552–563; E. Coronado, M. Clemente-León, J. R. Galán-Mascarós, C. Giménez-Saiz, C. J. Gómez-García, E. Martínez-Ferrero, *J. Chem. Soc. Dalton Trans.* **2000**, 3955–3961.
- [2] O. Waldmann, R. Koch, S. Schromm, P. Müller, I. Bernt, R. W. Saalfrank, *Phys. Rev. Lett.* **2002**, *89*, 246401-1-4.
- [3] Recent reviews: F. Hof, S. L. Craig, C. Nuckolls, J. Rebek, Jr., *Angew. Chem.* **2002**, *114*, 1556–1578; *Angew. Chem. Int. Ed.* **2002**, *41*, 1488–1508; B. J. Holliday, C. A. Mirkin, *Angew. Chem.* **2001**, *113*, 2076–2097; *Angew. Chem. Int. Ed.* **2001**, *40*, 2022–2043; S. R. Seidel, P. J. Stang, *Acc. Chem. Res.* **2002**, *35*, 972–983; R. W. Saalfrank, B. Demleitner, in *Transition Metals in Supramolecular Chemistry* (Ed.: J. P. Sauvage), Wiley-VCH, Weinheim, **1999**, pp. 1–51; D. L. Caulder, K. N. Raymond, *Acc. Chem. Res.* **1999**, *32*, 975–982; J. L. Atwood, L. R. MacGillivray, *Angew. Chem.* **1999**, *111*, 1080–1096; *Angew. Chem. Int. Ed.* **1999**, *38*, 1018–1033; M. Fujita, *Chem. Soc. Rev.* **1998**, *27*, 417–425; C. J. Jones, *Chem. Soc. Rev.* **1998**, *27*, 289–299; R. W. Saalfrank, B. Demleitner, N. Löw, S. Trummer, S. Kareth, *Mol. Cryst. Liq. Cryst.* **2001**, *356*, 71–90; G. F. Swiegers, T. J. Malefetse, *Coord. Chem. Rev.* **2002**, *225*, 91–121; M. D. Ward, J. A. McCleverty, J. C. Jeffery, *Coord. Chem. Rev.* **2001**, *222*, 251–272; V. L. Pecoraro, A. J. Stemmler, B. R. Gibney, J. J. Bodwin, H. Wang, J. W. Kampf, A. Barwinski, *Prog. Inorg. Chem.* **1997**, *45*, 83–177; J. A. R. Navarro, J. M. Salas, M. Quirós, M. Willermann, B. Lippert, *Chem. Eur. J.* **2003**, *9*, 4414–4421.
- [4] E. Uller, B. Demleitner, I. Bernt, R. W. Saalfrank, *Struct. Bonding* **2000**, *96*, 149–175.
- [5] Compare: A. Caneschi, A. Cornia, A. C. Fabretti, D. Gatteschi, *Angew. Chem.* **1999**, *111*, 1372–1374; *Angew. Chem. Int. Ed.* **1999**, *38*, 1295–1297; S. P. Watton, P. Fuhrmann, L. E. Pence, A. Caneschi, A. Cornia, G. L. Abbati, J. S. Lippard, *Angew. Chem.* **1997**, *109*, 2917–2919; *Angew. Chem. Int. Ed.* **1997**, *36*, 2774–2776; J. van Slageren, R. Sessoli, D. Gatteschi, A. A. Smith, M. Helliwell, R. E. P. Winpenny, A. Cornia, A.-L. Barra, A. G. M. Jansen, E. Rentschler, G. A. Timco, *Chem. Eur. J.* **2002**, *8*, 277–285.
- [6] R. W. Saalfrank, I. Bernt, E. Uller, F. Hampel, *Angew. Chem.* **1997**, *109*, 2596–2599; *Angew. Chem. Int. Ed. Engl.* **1997**, *36*, 2482–2485; R. W. Saalfrank, I. Bernt, F. Hampel, *Angew. Chem.* **2001**, *113*, 1745–1748; *Angew. Chem. Int. Ed.* **2001**, *40*, 1700–1703; R. W. Saalfrank, I. Bernt, F. Hampel, *Chem. Eur. J.* **2001**, *7*, 2770–2774.
- [7] Crystal structure analysis data for $[\text{Fe}_6\text{Cl}_6(\text{L}^1)_6]$ (**4**): $\text{C}_{114}\text{H}_{186}\text{Cl}_6\text{Fe}_6\text{N}_6\text{O}_{12}\cdot 6\text{toluene}$, $M_r=2933.29$; crystal dimensions $0.25 \times 0.25 \times 0.25 \text{ mm}^3$; rhombohedral, space group $R\bar{1}$, $a=33.778(5)$, $c=13.684(3) \text{ \AA}$, $V=13521(4) \text{ \AA}^3$; $Z=3$; $F(000)=4698$, $\rho_{\text{calcd}}=1.081 \text{ Mg m}^{-3}$; Diffractometer: Nonius KappaCCD area detector, $\text{Mo}_{\text{K}\alpha}$ radiation ($\lambda=0.71073 \text{ \AA}$); $T=173(2) \text{ K}$; graphite monochromator; theta range $[\circ]$ $1.21 < \theta < 27.53$; index range: $-39 \leq h \leq 43$, $-43 \leq k \leq 38$, $-17 \leq l \leq 16$; 2814 reflections measured, of which 2323 were independent and 1565 observed with $I > 2\sigma(I)$; linear absorption coefficient 0.609 mm^{-1} . The structure was solved by direct methods using SHELXS-97 and refinement with all data (245 parameters) by full-matrix least-squares on F^2 using SHELXL97^[8]; all non-hydrogen atoms were refined anisotropically; $R1=0.1225$ for $I > 2\sigma(I)$ and $wR2=0.3542$ (all data); largest peak $=1.180 \text{ e\AA}^{-3}$ and hole $=-0.629 \text{ e\AA}^{-3}$ ^[8,9]
- [8] G. M. Sheldrick, C. Krüger, P. Goddard, *Crystallographic Computing 3*, Oxford University Press, Oxford **1985**, p. 175; G. M. Sheldrick, SHELXL-97, Program for Crystal Structure Refinement, University of Göttingen **1997**.
- [9] CCDC-211210 (**4**), CCDC-211209(**5**) and CCDC-222750 (**7**) contain the supplementary crystallographic data (excluding structure factors) for this paper. These data can be obtained free of charge via www.ccdc.cam.ac.uk/const/retrieving.html (or from the Cambridge Crystallographic Data Centre, 12, Union Road, Cambridge CB21EZ, UK; fax: (+44)1223-336-033; or deposit@ccdc.cam.ac.uk).
- [10] Crystal structure analysis data for $[\text{In}_6\text{Cl}_6(\text{L}^1)_6]$ (**5**): $\text{C}_{114}\text{H}_{186}\text{Cl}_6\text{In}_6\text{N}_6\text{O}_{12}\cdot 6\text{THF}$, $M_r=3166.93$; crystal dimensions $0.20 \times 0.20 \times 0.20 \text{ mm}^3$; rhombohedral, space group $R\bar{1}$, $a=34.283(5)$, $c=13.640(3) \text{ \AA}$, $V=13883(4) \text{ \AA}^3$; $Z=3$; $F(000)=4932$, $\rho_{\text{calcd}}=1.136 \text{ Mg m}^{-3}$; Diffractometer: Nonius KappaCCD area detector, $\text{Mo}_{\text{K}\alpha}$ radiation ($\lambda=0.71073 \text{ \AA}$); $T=173(2) \text{ K}$; graphite monochromator; theta range $[\circ]$: $2.89 < \theta < 27.52$; index range: $-37 \leq h \leq 44$, $-44 \leq k \leq 37$, $-15 \leq l \leq 15$; 3058 reflections measured, of which 2638 were independent and 1765 observed with $I > 2\sigma(I)$; linear absorption coefficient 0.870 mm^{-1} . The structure was solved by direct methods using SHELXS-97 and refinement with all data (262 parameters) by full-matrix least-squares on F^2 using SHELXL-97^[8]; all non-hydrogen atoms were refined anisotropically; $R1=0.0649$ for $I > 2\sigma(I)$ and $wR2=0.1936$ (all data); largest peak $=0.556 \text{ e\AA}^{-3}$ and hole $=-0.385 \text{ e\AA}^{-3}$ ^[8,9]
- [11] For dynamic NMR spectroscopy see: R. W. Saalfrank, B. Demleitner, H. Glaser, H. Maid, D. Bathelt, F. Hampel, W. Bauer, M. Teichert, *Chem. Eur. J.* **2002**, *8*, 2679–2683; R. W. Saalfrank, B. Demleitner, H. Glaser, H. Maid, S. Reihls, W. Bauer, M. Maluenga, F. Hampel, M. Teichert, H. Krautscheid, *Eur. J. Inorg. Chem.* **2003**, 822–829; S. Hiraoka, K. Harano, T. Tanaka, M. Shiro, M. Shionoya, *Angew. Chem.* **2003**, *115*, 5340–5343; *Angew. Chem. Int. Ed.* **2003**, *42*, 5182–5185.
- [12] For movies visualizing the dynamics of $(\Delta\Delta\Delta\Delta)$ - $\{(\text{NH}_4)_4[\text{Mg}_4(\text{L})_6]\}^{\pm}(A_1A_1A_1A_1)-\{(\text{NH}_4)_4[\text{Mg}_4(\text{L})_6]\}$ and $S_6\text{-}5\text{e}^-\text{S}_6\text{-}5'$ see <http://www.organik.uni-erlangen.de/saalfrank/>.
- [13] Gaussian 98, Revision A.11.3, M. J. Frisch, G. W. Trucks, H. B. Schlegel, G. E. Scuseria, M. A. Robb, J. R. Cheeseman, V. G. Zakrzewski, J. A. Montgomery, Jr., R. E. Stratmann, J. C. Burant, S. Dapprich, J. M. Millam, A. D. Daniels, K. N. Kudin, M. C. Strain, O. Farkas, J. Tomasi, V. Barone, M. Cossi, R. Cammi, B. Mennucci, C. Pomelli, C. Adamo, S. Clifford, J. Ochterski, G. A. Petersson, P. Y. Ayala, Q. Cui, K. Morokuma, N. Rega, P. Salvador, J. J. Dannenberg, D. K. Malick, A. D. Rabuck, K. Raghavachari, J. B. Foresman, J. Cioslowski, J. V. Ortiz, A. G. Baboul, B. B. Stefanov, G. Liu, A. Liashenko, P. Piskorz, I. Komaromi, R. Gomperts, R. N. Martin, D. J. Fox, T. Keith, M. A. Al-Laham, C. Y. Peng, A. Nanayakkara, M. Challacombe, P. M. W. Gill, B. Johnson, W. Chen, M. W. Wong, J. L. Andres, C. Gonzalez, M. Head-Gordon, E. S. Replogle, J. A. Pople, Gaussian, Inc., Pittsburgh PA, **2002**.
- [14] A. D. Becke, *J. Phys. Chem.* **1993**, *97*, 5648–5652; P. J. Stephens, F. J. Devlin, C. F. Chabalowski, M. J. Frisch, *J. Phys. Chem.* **1994**, *98*, 11623–11627.
- [15] T. H. Dunning, Jr., P. J. Hay, *Mod. Theor. Chem.* **1976**, *3*, 1–28; P. J. Hay, W. R. Wadt, *J. Chem. Phys.* **1985**, *82*, 270–283; P. J. Hay, W. R. Wadt, *J. Chem. Phys.* **1985**, *82*, 284–298; P. J. Hay, W. R. Wadt, *J. Chem. Phys.* **1985**, *82*, 299–310.
- [16] *Gaussian Basis Sets for Molecular Calculations* (Ed.: S. Huzinaga), Elsevier, Amsterdam, **1984**.
- [17] Turbomole, a program package for ab initio electronic structure calculations, copyright **1988–2002** Prof. Dr. Reinhart Ahlrichs, Institut für Physikalische Chemie und Elektrochemie, Universität Karlsruhe.
- [18] A. D. Becke, *Phys. Rev. A* **1988**, *38*, 3098–3100; J. P. Perdew, *Phys. Rev. B* **1986**, *33*, 8822–8824.
- [19] K. Eichkorn, O. Treutler, H. Öhm, M. Häser, R. Ahlrichs, *Chem. Phys. Lett.* **1995**, *240*, 283–290; K. Eichkorn, F. Weigand, O. Treutler, R. Ahlrichs, *Theor. Chem. Acc.* **1997**, *97*, 119–124.
- [20] A. Schäfer, H. Horn, R. Ahlrichs, *J. Chem. Phys.* **1992**, *97*, 2571–2577.

- [21] Cf.: C. J. Hawker, K. L. Wooley, J. M. J. Fréchet, *J. Chem. Soc. Dalton Trans.* **1993**, 1, 1287–1297.
- [22] Crystal structure analysis data for $[\text{Fe}_6(\text{SCN})_6(\text{L}^3)_6]$ (**7**): $\text{C}_{180}\text{H}_{186}\text{Fe}_6\text{N}_6\text{O}_{48}\text{S}_6 \cdot 3\text{CHCl}_3 \cdot 2\text{Et}_2\text{O}$, $M_r = 4557.95$; crystal dimensions $0.25 \times 0.08 \text{ mm}^3$; triclinic, space group $P\bar{1}$, $a = 13.1839(2)$, $b = 20.4576(4)$, $c = 21.1174(4) \text{ \AA}$, $\alpha = 98.428(2)$, $\beta = 102.778(2)$, $\gamma = 100.189(2)^\circ$, $V = 5363.7(2) \text{ \AA}^3$; $Z = 1$; $F(000) = 2360$, $\rho_{\text{calcd}} = 1.411 \text{ Mg m}^{-3}$; Diffractometer: Nonius KappaCCD area detector, $\text{MoK}\alpha$ radiation ($\lambda = 0.71073 \text{ \AA}$); $T = 100(2) \text{ K}$; graphite monochromator; theta range $[\circ]$: $3.71 < \theta < 25.03$; index range: $-15 \leq h \leq 15$, $-24 \leq k \leq 24$, $-25 \leq l \leq 25$; 3058 reflections measured, of which 18788 were independent and 12421 observed with $I > 2\sigma(I)$; linear absorption coefficient 0.718 mm^{-1} . The structure was solved by direct methods using SHELXTL NT 6.12 and refinement with all data (1334 parameters) by full-matrix least-squares on F^2 using SHELXL 97;^[8] all non-hydrogen atoms were refined anisotropically; $R1 = 0.0763$ for $I > 2\sigma(I)$ and $wR2 = 0.2281$ (all data); largest peak = $1.278 \text{ e}\text{\AA}^{-3}$ and hole = $-0.987 \text{ e}\text{\AA}^{-3}$.^[8,9]
- [23] M. Kawa, J. M. J. Fréchet, *Chem. Mater.* **1998**, 10, 286–296; J. M. J. Fréchet, *Proc. Natl. Acad. Sci. USA* **2002**, 99, 4782–4787.
- [24] R. W. Saalfrank, I. Bernt, M. M. Chowdhry, F. Hampel, G. M. M. Vaughan, *Chem. Eur. J.* **2001**, 7, 2765–2769.

Received: June 1, 2003

Revised: December 19, 2003 [F 6050]